ADVANTAGES OF USING PLANE POLISHED SECTION ANALYSIS AS PART OF MICROSTRUCTURAL ANALYSES TO DESCRIBE INTERNAL CRACKING DUE TO ALKALI-SILICA REACTIONS

Jan Lindgård [1*], Marit Haugen [1], Nelia Castro [2], Michael D.A. Thomas [3]

[1]SINTEF Building and Infrastructure, Trondheim, NORWAY

[2]Norwegian University of Science and Technology, NO-7491 TRONDHEIM, Norway

[3]University of New Brunswick, Fredericton, CANADA

Abstract

Microstructural analysis is an important tool to diagnose and describe the extent of any ASR in concrete structures. Such analysis is additionally recommended to be performed in connection with laboratory testing of alkali reactivity to confirm that measured expansions are caused by ASR.

In a separate paper, a PhD study of the principal author on ASR performance testing is described. In order to confirm presence and extent of ASR after the exposure, microstructural analyses have been performed. These examinations included analysis of plane polished and thin sections, as well as SEM analysis. By using image analysis, the crack patterns in the plane polished sections were analysed to quantify the extent and distribution of cracks in concrete prisms. This paper presents some important findings from the microstructural analyses, with focus on the advantages of using plane polished section analysis as part of microstructural analysis to describe internal cracking due to ASR.

Keywords: alkali silica reaction, microstructural analysis, image analysis

1 INTRODUCTION

1.1 Background

Microstructural analysis as part of a condition survey

At SINTEF, microstructural analysis is a very important tool to diagnose and describe the extent of any ASR in a concrete structure. Such analysis includes macroscopic examination of fluorescent impregnated plane polished sections (in ordinary light and UV-light), examination of thin sections in a polarization microscope (with and without fluorescence filter) and occasionally Scanning Electron Microscopy (SEM) analysis, as well. The crack patterns are of particular importance in the ASR diagnosis.

Many petrographers only use microstructural analyses (i.e. analysis of thin sections and SEM) in their examinations. These analyses give a very good view of details in the interior of a structure, but they are less suited to give a sufficient overview of the extent of cracking in the concrete.

At SINTEF, more than 20 years of experiences have shown the importance and advantages of using larger samples to describe the crack intensity and crack pattern in drilled concrete cores by analysis of plane polished sections. Thus, a better correlation to what is observed in the field might be obtained. However, the presumption is that an experienced person performs the field survey, in addition to selecting representative

* Correspondence to: jan.lindgard@sintef.no

sampling locations on the structures. It is also important to carry out a comprehensive visual examination of the drilled cores when they arrive in the laboratory as a basis for detail planning of the laboratory program.

Normally, several complementary laboratory analyses are part of a survey of concrete structures with possible ASR damage, e.g. moisture state and mechanical properties (compressive strength and E-modulus).

Microstructural analysis as part of ASR laboratory testing

Several concrete prism tests (CPTs), e.g. RILEM AAR-3 [1], recommend that microstructural examinations are performed in connection with laboratory testing of alkali reactivity. If the expansion is judged to be deleterious, it is recommended to examine the internal features and crack patterns to confirm that the expansion is caused by ASR.

Description of the extent of internal cracking in concrete samples

In Canada, the DRI method developed by Dr. P.E. Grattan-Bellew [2] is frequently used to quantify internal deterioration caused by ASR. The method makes use of plane polished sections, but without impregnating them with any fluorescence. In the analysis, the following parameters are counted: cracks, precipitation of alkali gel, de-bonding and reaction rims. The different parameters are weighted as basis for calculating the DRI, i.e. a number describing the degree of damage in the plane polished section.

In Norway, the DRI method is rarely used, even though quantification of internal cracking has high focus. Instead, the extent of cracking is described verbally, in addition to describing type of cracks; e.g. whether cracks are running from the aggregates and into the cement paste, whether cracks connect aggregate particles or whether cracks appear parallel to the concrete surface (might indicate freeze/thaw damage). A more simple "cracking index" has, however, been used in a previous research project [3].

PhD study on performance testing – post-documentation of concrete prisms

In a separate paper [4], a PhD study of the principal author on laboratory ASR performance testing is described. A main aim of the PhD study, being part of the Norwegian COIN project (www.coinweb.no), has been to evaluate whether CPTs developed for assessment of alkali-silica reactivity of aggregates might be suitable for general ASR performance testing of concrete. In order to confirm the presence and extent of ASR after the exposure, microstructural analyses have been performed on selected concrete prisms. These examinations have included analysis of plane polished sections and thin sections, as well as SEM analysis.

The extent of internal cracking in the concrete prisms is documented in the plane polished sections that cover the whole prism (70x280 mm). In the photos taken in UV-light crack patterns appear clearly. By use of image analysis, the crack patterns were analysed to quantify the extent and spread in cracking in the concrete prisms. The image analysis is used as an alternative to the more time consuming DRI method [2].

This paper presents some important findings from the microstructural analyses, with focus on the advantages of using plane polished section analysis as part of microstructural analysis to describe internal cracking due to ASR.

2 THE TEST PROGRAMME

2.1 General

Of the 60 test series included in the PhD study [4], one prism from each of 15 test series was analysed by microstructural analysis after the ASR exposure in order to examine the presence and extent of ASR. The prisms were carefully selected to cover a wide range of concrete types and ASR exposure conditions, as well as a spread in expansion. Additionally, the visual descriptions were helpful in the selection.

In total 16 fluorescence impregnated polished sections were prepared (two polished sections were needed for the larger Norwegian concrete prism, 100x100x450 mm). From the same prisms, 25 fluorescence impregnated and polished thin sections for optical polarization microscopy were additionally prepared. 11 of these were also analysed by SEM.

2.2 Visual description

After the ASR exposure, one prism from each of the 60 test series was described visually. At first, any surface cracking and precipitation were registered and photographed. As part of further analyses of the prisms, each prism was cut in several pieces by use of a splitter [4]. Secondly, the cut faces of the prism ends were carefully examined to search for any internal gel exudation in cracks and pores.

2.3 Plane polished section analysis

In addition to give a general description of the extent of cracking and crack patterns in the 16 plane polished sections, the observed crack features were documented by taking photos in normal light and UV light. Examples of such photos are shown in Figure 1 and 2.

Measurement of cracking intensity by image analysis

In this study, the program Image SXM [5], a public domain image processing and analysing software, was used to create maps of the cracks in the polished sections through thresholding of the grey level histogram. The input images were acquired in fluorescent light, so the cracks were easily differentiated from the aggregates and the cement paste (Figure 2). The careful image acquisition (Figure 3) guaranteed that the brightness and contrast were reproducible and that the corresponding digital pixel values were stable. Thus, it was possible to use a fixed grey level threshold, effectively automating this step. A few images required additional minor manual corrections to erase relics of air voids that were not effectively avoided in the thresholding since their grey levels overlapped the crack's grey levels. After segmentation, the total *Area%* occupied by the cracks in each image, defined as the "cracking intensity", was analysed. This measure was further used to compare the cracking intensity in the various plane polished sections.

The prisms were stored with the same end facing upwards during the whole exposure time [4]. To measure any spread in internal cracking intensity over the prisms, the segmented images were divided in crosswise slices of 25 mm or lengthwise slices of 14 mm (12.5 mm in the larger Norwegian prisms) and the *Area%* occupied by the cracks in each slice was analysed. The values obtained for each slice were then normalized to the total *Area%*.

2.4 Thin section analysis

The 25 fluorescence impregnated thin sections were examined in a polarization microscope with a UV-filter. The following parameters were analysed: any reacting aggregate particles, any cracking, any precipitations (e.g. of ASR gel), porosity (w/cm ratio), distribution and size of air voids and any dissolution. During the analysis, emphasis was put on describing presence and extent of ASR by evaluating the amount of alkali-silica gel and the extent and location of cracks.

2.5 SEM analysis

The backscattered electron imaging (BEI) mode in SEM gives a picture of the different phases in the sample as a range of grey values [6]. The 11 samples analysed in the study were sputtered with carbon under vacuum to make them conductive before inspection by SEM. In addition to a brief visual examination of the

polished thin sections, the composition of any precipitations (primarily ASR gel) was analysed by EDS (Energy Dispersive Spectrum of X-rays) or WDS (wavelength dispersive X-ray spectrometer).

Measurement of remaining alkali content

During an accelerated ASR laboratory test, the extent of alkali leaching and the depth influenced by alkali leaching is of importance for the prism expansion [7], [8]. In the PhD study, the extent of alkali leaching was documented by analysing the content of alkalis accumulated in the water in the bottom of each storage container [4]. Additionally, it was of interest to measure the remaining alkali content within the concrete prisms, but it is very difficult, maybe impossible, to squeeze out pore water from a concrete with a w/c ratio < 0.50, as applied for most test series. Alternative measuring procedures were thus included in the study.

To try to detect the depths influenced by alkali leaching and to check if any correlation exists between calculated remaining alkali content in the prisms and the extent of alkali leaching, WDS analysis was used in combination with the SEM analysis of the 11 polished thin sections. The content of alkalis, Na and K, in the binder was measured continuously from the outer surface to the centre of the prisms.

3 RESULTS

In this paper, only selected results from analyses of the plane polished sections are presented, with focus on description and quantification of the extent of internal cracking.

3.1 Visual description

The extent of surface cracking varied hugely between prisms exposed to various exposure conditions during the ASR performance testing and thus revealed different expansions [4]. The unwrapped prisms exposed to 60°C revealed the most extensive surface precipitation compared with corresponding prisms exposed to 38°C. Hardly any precipitation was registered on the surfaces of the prisms wrapped in damp cotton cloth and polyethylene according to the description in the RILEM AAR-3 CPT (2000) [9].

After splitting the prisms, white precipitation was observed in air voids in many of the samples, in particular in the prisms from the test series with highest expansion. An extensive content of such precipitation was also observed in many prisms after four weeks of exposure to 60°C.

3.2 Plane polished section analysis

Extent of cracking

The analyses of the plane polished sections showed a huge spread in extent of cracking, both internally within some of the prisms and between prisms from various test series. One example of the former is shown in Figure 2, showing a UV-photo of a prism from a test series with a relatively porous binder (CEM I, w/c 0.60) exposed to 100 % relative humidity (RH) and 60°C for 39 weeks. All prisms were stored with the same end facing upwards (right side of the picture) during the whole exposure time. As can be seen, the extent of cracking is low in the lower (0-30 mm) and the upper (80-100 mm) sections, while the medium section is rather heavily cracked. The 39-week expansion for this prism was measured to be 0.18 %.

Other examples, showing rather extensive cracking over a larger area of the prism is given in Figures 4 and 5. Figure 4 shows the UV-photo of a prism from a test series with a more dense binder (CEM I, w/c 0.45) exposed to 100 % RH and 38°C for 2 years, revealing a 2-years expansion of 0.30 %. Also for this prism the extent of cracking is somewhat less in the bottom and upper sections. Figure 5 shows the UV-photo of the lower part of a prism from a test series with a similar binder exposed to similar conditions for 2 years, but with larger prism size (100 mm cross sections instead of 70 mm). This prism revealed a 2-years expansion of 0.43 %. The cracks seem to be rather homogenously distributed in the prism.

Measurement of cracking intensity by image analysis

Results from the measurements of total cracking intensity (*Area%*) by image analysis of the 16 plane polished sections are presented in Figure 6. In this figure, the cracking intensities are plotted against the measured prism expansions. In all 16 prisms, the same aggregate combination, but four different binders (CEM I with three w/c ratios ranging from 0.30 to 0.60 and a CEM II-A/V fly ash cement with w/c ratio 0.45) were used.

Results from measurements of relative cracking intensity lengthwise from the bottom to the top of the prisms (the prisms were stored in this positions during the whole exposure time), after dividing each prism in crosswise slices of 25 mm, are shown in Figure 7 and 8.

Results from measurements of cracking intensity crosswise, after dividing each of the prisms in five lengthwise slices of 14 mm, are shown in Figure 9.

3.3 Thin section analysis

The analyses detected ASR in all the 25 examined thin sections. The extent of cracking varies, as well as the amount of alkali-silica gel present in air voids and cracks. The alkali-reactive Norwegian cataclasite has reacted in all the 16 test series examined by thin sectioning. However, no particles in the Årdal sand, classified as non-reactive according to the Norwegian ASR regulations [10], have shown any sign of reaction.

3.4 SEM analysis

The SEM analyses showed alkali-silica gel in all the 11 examined samples, occurring in air voids, in cracks in the cement paste, sometimes distributed within the cement paste, in the interface between aggregate particles and the cement paste or in cracks within the aggregate particles. The composition of the alkali-silica gel varied somewhat depending on the location within the concrete. As referred by several others [8], the alkali-silica gel tends to exchange alkalis with calcium when moving from the cracks inside an aggregate and out in the cement paste. Additionally, the extent of cracking in the thin sections varied.

4 DISCUSSION

Post-documentation after the ASR exposure – use of various analysing techniques

During the introductory visual examinations in the laboratory, the concrete samples were carefully checked as a basis to plan which samples were to be used for which analysis. During the preparation of the plane polished and thin sections, the first step was to saw the samples into two longitudinally halves. One half was used for preparation of the plane polished section, while one or two thin sections were prepared from the other half in locations where alkali-silica gel seemed to occur. As can be seen from Figure 2, the selected locations of the thin sections, only covering very limited parts of the concrete prisms, has a very high influence on the outcome and conclusion of the thin section analysis.

The thin section and SEM analyses documented as expected alkali-silica reactions to be the cause of expansion of the 16 concrete prisms examined after the ASR exposure. Even though these investigations are important tools to document that ASR really is the cause of expansion, none of these analysing techniques are well suited to assess the extent and variation in damage within larger concrete samples. For such evaluations, detection of crack pattern in plane polished sections gives a much better overview of the degree of damage, e.g. as shown in Figure 2, 4 and 5. However, the microscopy techniques are important tools for diagnosis and for detailed examinations, e.g. for measurement of the composition of alkali-silica gel by applying EDS or WDS analysis as part of the SEM analysis. The WDS analyses showed for instance that for various binders and both exposure temperatures (38 and 60°C), the alkali-silica gel picks up calcium (exchanged with Na and K) when moving from the cracks inside an aggregate and out in the cement paste.

Measurement of cracking intensity by image analysis

Image analysis is a less time consuming analysing technique compared with the DRI method [2]. It is also not necessary to use a microscope. Similar to the DRI method, the outcome of the image analysis is a number, representing the degree of damage (*area%* of cracks) in a plane polished section. On the other hand, the DRI method involves more parameters connected to an alkali-silica reaction, i.e. reaction products, reaction rims and de-bounding. However, as long as the same aggregate composition has been used in all the test series and the detailed analysing techniques documented that ASR was the cause of expansion, the image analyses could successfully be used in order to compare the extent of cracking, both internally within one plane polished section and between different test series.

A pretty good linear correlation was found between the cracking intensity (given as area% of cracks in the plane polished sections) and the measured prism expansion (Figure 6), even though four different binder qualities were used. The 28 days compressive strength ranged from 44 to 103 MPa. The aggregate composition was, however, identical in all test series. The good correlation found indicates that the accuracy of the image analysing technique is sufficiently good to use the method as a tool to analyse the degree of ASR damage in larger concrete samples. Rivard and Ballivy [11] have also previously found a rather good correlation between the measured expansion caused by ASR on laboratory-concrete prisms and the damage to concrete, as quantified by the DRI on polished sections prepared from these prisms.

For field samples from different structures with varying aggregate composition, the crack patterns are assumed to vary widely. As a consequence, the correlation between the cracking intensity and expansion is assumed to be reduced. Rivard and Ballivy [11] state that "DRI values are not absolute, but are a relative indicator for a particular aggregate or aggregate-cement combination of the extent of ASR damage". In most parts of a real concrete structure, the concrete is not free to expand, a matter that also is assumed to influence the correlation between internal cracking and expansion.

The lengthwise measurements of cracking intensity from the bottom to the top of the prisms, after dividing each prism in crosswise slices of 25 mm (Figure 8 and 9), show that the upper 25 mm of the prisms exhibit least cracking for most test series, followed by the lower 25 mm of the prisms. Further, in most cases the slices located 25-50 mm from the top of the prisms revealed less cracking than the slices located in correspondent distance from the bottom of the prisms. The mid parts of the prisms revealed significantly higher expansion compared with the upper 50 mm and lower 25 mm of the prisms. However, for some samples, and in particular the test series with binder CEM I, w/c 0.60 exposed to 60°C (Figure 2), a larger area of the upper half of the prism has minor cracking compared with the mid parts.

Also the crosswise measurements of cracking intensity, after dividing each prism in lengthwise slices (Figure 9) show that the outer 10-15 mm of the prisms get somewhat less cracking compared with the interior of the prisms.

The main reason for lower extent of cracking in the outer/upper/lower parts of the prisms compared with the interior of the prisms is assumed to be alkali leaching. The preliminary results from measurement of rate and extent of alkali leaching have shown a good correlation between expansion and extent of alkali leaching [4]. Since alkali leaching is connected to diffusion of ions from the interior of the prisms to the wet concrete surface, it is assumed that more porous concretes will have higher tendency to leach out alkalis. It is thus reasonable that the sample showing the least crack intensity in the upper third of the prism compared with the mid part is the most porous one with the highest w/c (see Figure 2).

Three of the 11 thin sections examined by WDS analysis were located in the top of the prisms, while one thin section was located in the bottom of the prism. In the three thin sections from the top of the prisms the mean alkali content in the upper 15 mm was 30-40 % lower compared with the mean alkali content in distance 20-35 mm from the top. For the thin section located in the bottom of one prism, the mean alkali

content in the lower 15 mm was about 60 % lower compared with the mean alkali content in distance 20-35 mm from the bottom.

Of all the test methods included in the PhD study, the larger prisms used in the Norwegian CPT revealed highest expansion and least alkali leaching [4]. As can be seen in Figure 5, no distinct difference on cracking between outer and inner parts of the prism could be observed.

5 CONCLUSIONS

Based on microstructural analysis of 15 concrete prism test series after exposure to 100 % RH and 38 or 60°C, the following conclusions may be drawn:

- Image analysis could successfully be used in order to compare extent of cracking due to ASR in the concretes (with identical aggregate composition, but various binder qualities), both internally within one plane polished section and between different test series.
- A pretty good linear correlation was found between the cracking intensity (given as area% of cracks in the plane polished sections) and the measured prism expansion. The good correlation found indicates that the accuracy of the image analysing technique is sufficient good to use the method as a tool to analyse the degree of ASR damage in larger concrete samples.
- The main reason for lower extent of cracking in the outer/upper/lower parts of the prisms compared with the interior of the prisms is assumed to be alkali leaching.

6 REFERENCES

[1] RILEM TC 219-ACS (2011): 'Alkali-silica reactions in Concrete Structures': RILEM recommended test method: Detection of potential alkali-reactivity - 38°C test method for aggregate combinations using concrete prisms, (unpublished draft).

[2] Grattan-Bellew, PE, Danay, A (1992): Comparison of laboratory and field evaluation of alkali-silica reaction in large dam, in: International Conference on Concrete AAR in Hydroelectric Plants and Dams, Canadian Electrical Association in association with Canadian National Committee of ICOLD, Fredericton, Canada, pp. 23.

[3] Lindgård, J, Skjølsvold, O, Haugen, M (2004): Experience from evaluation of degree of damage in fluorescent impregnated plane polished sections of half-cores based on the "Crack index method", in: M. Tang, M. Deng (Eds.) 12th International Conference on Alkali-Aggregate Reactions in Concrete, Beijing, China, pp. 939-947.

[4] Lindgård, J, Rønning, TF, Thomas, MDA (2012): Development on an ASR performance test: preliminary result from a PhD study, in: 14th International Conference on Alkali-Aggregate Reactions in Concrete (submitted proceedings), Austin, Texas.

[5] Barret, SD (2008): Image SXM: http://www.ImageSXM.org.uk.

[6] Scrivener, KL (2004): Backscattered electron imaging of cementitious microstructures: understanding and quantification, Cement and Concrete Composites, (26) 935-945.

[7] Lindgård, J, Andiç-Çakır, Ö, Borchers, I, Broekmans, MTAM, Brouard, E, Fernandes, I, Giebson, C, Pedersen, B, Pierre, C, Rønning, TF, Thomas, MDA, Wigum, BJ (2011): RILEM TC219-ACS-P: Literature survey on performance testing, COIN project report 27, ISBN: 978-82-536-1209-6, pp. 164.

[8] Lindgård, J, Andiç-Çakır, Ö, Fernandes, I, Rønning, TF, Thomas, MDA (2011): Alkali-silica reactions (ASR): Literature review on parameters influencing laboratory performance testing, Cement and Concrete Research, in press.

[9] RILEM TC 106-AAR (2000): 'Alkali Aggregate Reaction' A. TC 106-2- Detection of Potential Alkali-Reactivity of Aggregates –The Ultra-Accelerated Mortar-Bar Test B. TC 106-3-Detection of Potential Alkali-Reactivity of Aggregates-Method for Aggregate Combinations Using Concrete Prisms, Materials and Structures, (33) 283-293.

[10] Norwegian Concrete Association (2004): Durable concrete containing alkali reactive aggregates, NB21, pp. 33.

[11] Rivard, P, Ballivy, G (2005): Assessment of the expansion related to alkali-silica reaction by the Damage Rating Index method, Construction and Building Materials, (19) 83-90.

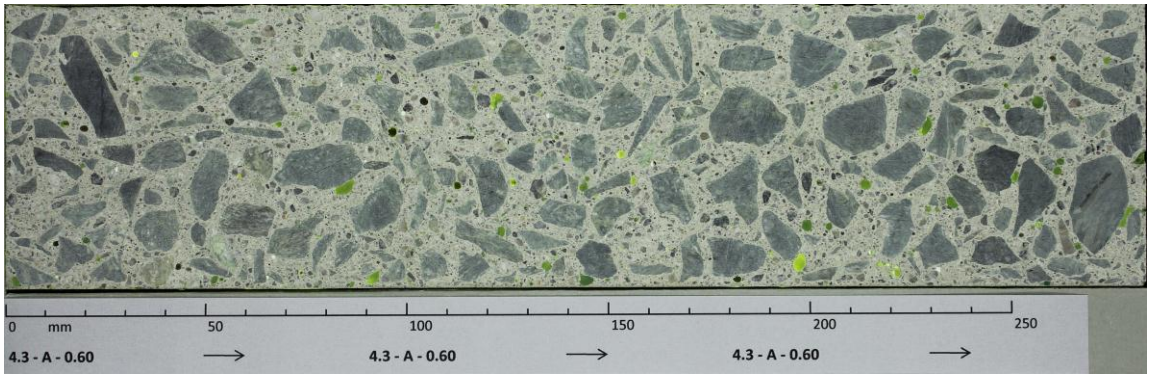

FIGURE 1: Photo in normal light of the plane polished section from test series 4.3-A-0.60.

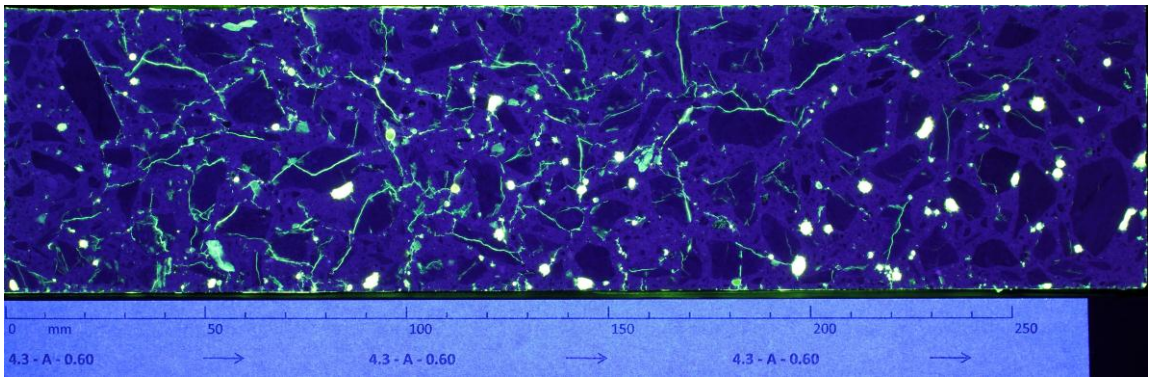

FIGURE 2: Photo in UV-light of the plane polished section shown in Figure 1.

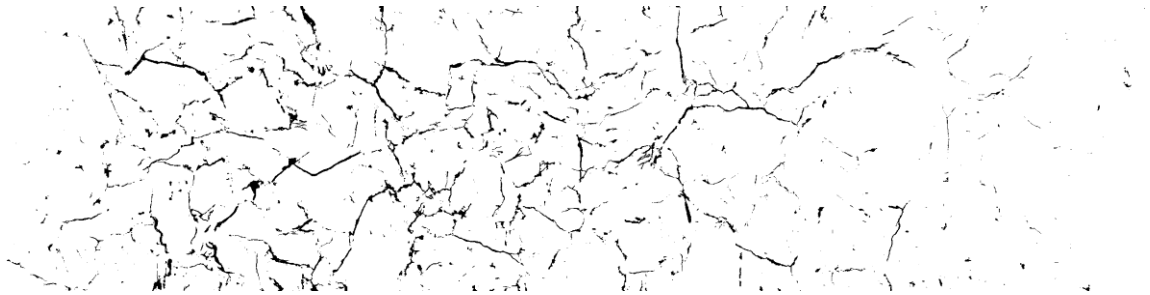

FIGURE 3: Map of the cracks in the plane polished section shown in Figure 1 and 2.

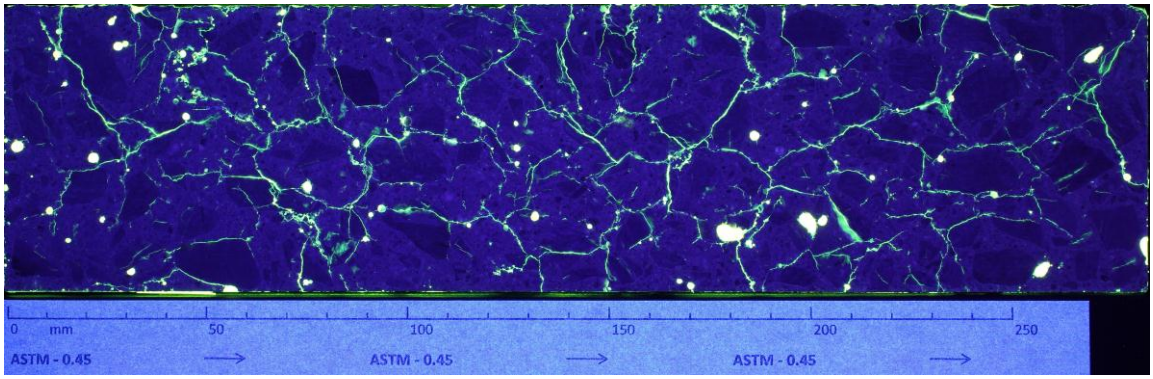

FIGURE 4: Photo in UV-light of the plane polished section from test series ASTM-0.45.

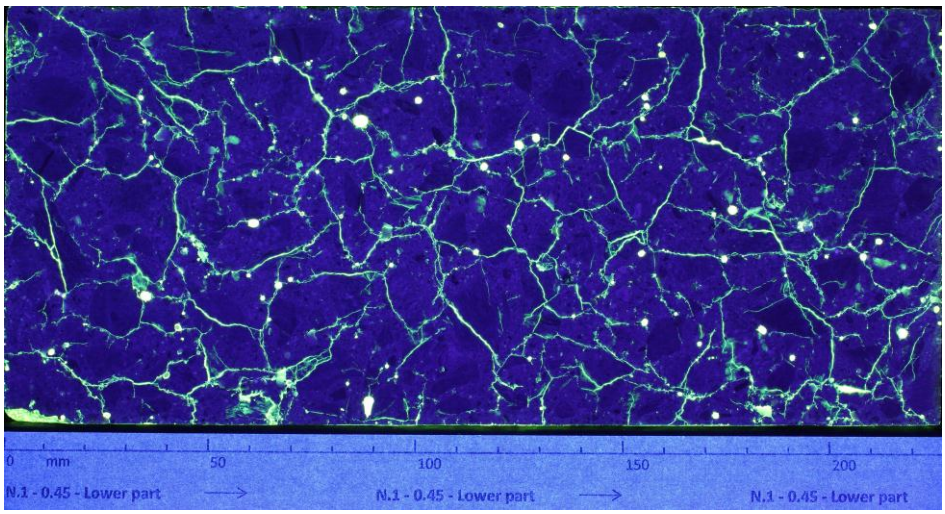

FIGURE 5: Photo in UV-light of the plane polished section from test series N1-0.45.

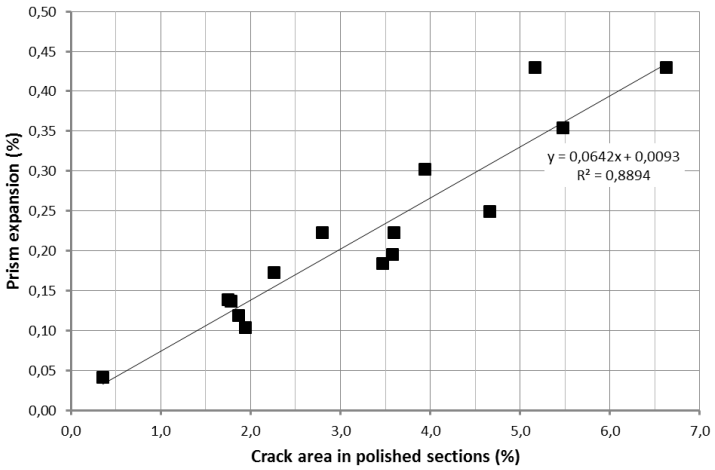

FIGURE 6: Total cracking intensity (Area%) in the 16 plane polished sections plotted against the measured prism expansions.

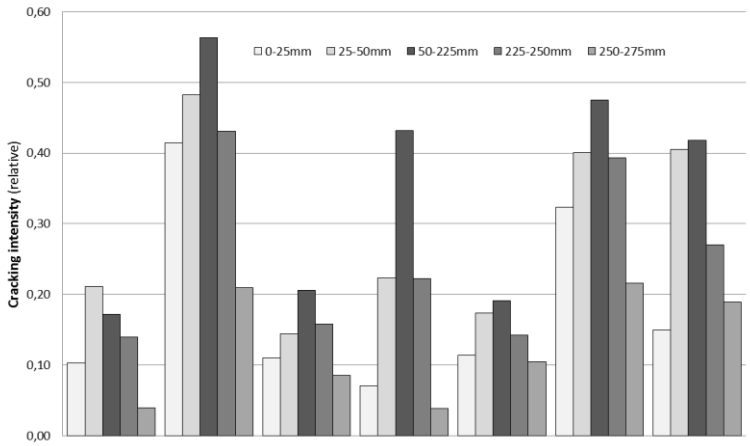

FIGURE 7: Relative cracking intensities in seven polished sections vs. height from the bottom (CEM I, w/c ratio 0.30 or 0.45, exposed to 38°C for 52 or 112 weeks). The test series to the right is the prism shown in Figure 4.

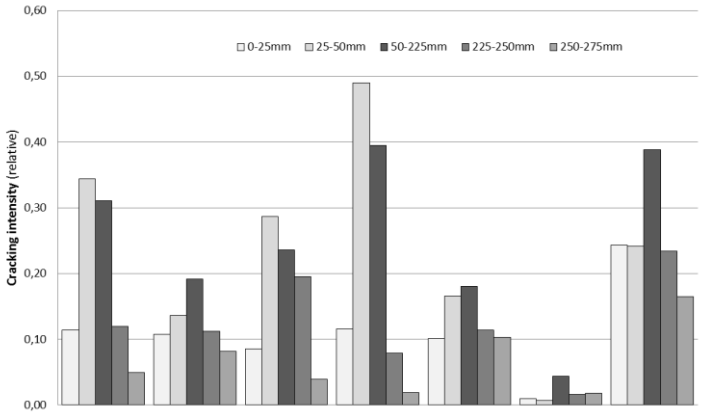

FIGURE 8: Relative cracking intensities in seven polished sections vs. height from the bottom (CEM I, w/c ratio ranging from 0.30 to 0.60, exposed to 60°C for 39 weeks). The test series in the middle is the prism shown in Figure 2.

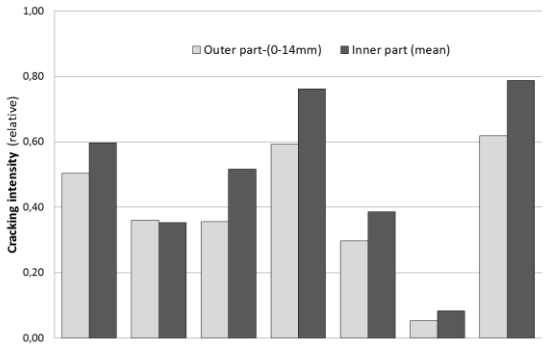

FIGURE 9: Relative cracking intensities in the same seven polished sections as shown in figure 8, but calculated crosswise, after dividing each of the prisms in five lengthwise slices of 14 mm. The test series in the middle is the prism shown in Figure 2.